JOURNAL OF Materials CHEMISTRY

Electrochemical sodium insertion/extraction in $Na_2(MoOPO_4)_2(HPO_4)\cdot yH_2O$ ($y=2, 0$)†

L. Mesonero Herrero,[a,b] M. E. Arroyo y de Dompablo,[b] M. J. Ruiz Aragón[b] and E. Morán*[b]

[a] *Laboratorio Complutense de Altas Presiones (LCAP), Facultad de Ciencias Químicas, Universidad Complutense, 28040 Madrid, Spain*
[b] *Departamento de Química Inorgánica, Facultad de Ciencias Químicas, Universidad Complutense, 28040 Madrid, Spain. E-mail: emoran@eucmax.sim.ucm.es*

Received 17th August 1998, Accepted 17th August 1998

The electrochemical sodium insertion and extraction of the phosphomolybdates $Na_2(MoOPO_4)_2(HPO_4)\cdot yH_2O$ ($y=2, 0$) is reported. Both compounds show a similar behaviour upon electrochemical sodium extraction, while the insertion reaction is notably different for each host compound. During the charge/discharge of electrochemical cells the existence of new phases $Na_{2+x}(MoOPO_4)_2(HPO_4)\cdot 2H_2O$ with compositions $-0.7<x<-0.4$, and $0.75<x<0.9$, as well as $Na_{2+x}(MoOPO_4)_2(HPO_4)$ with $-1<x<-0.75$ and $2.6<x<3.2$ has been detected. A member of each solid solution has been synthesised and preliminarily structurally characterised by powder X-ray diffraction. Although all of these new phosphomolybdates present a similar monoclinic structure, the unit cell volume increases progressively with the introduction of sodium and water in the tunnels. Magnetic susceptibility measurements have also been performed in order to follow the electrochemical process.

Introduction

Since many phosphomolybdates have layer structures or open crystalline lattices they can undergo redox reactions and therefore are potential candidates to be used in electrochemical devices such as batteries, displays and sensors. Such structures are unlikely to be thermally stable under traditional high-temperature solid state conditions, so that new low-temperature approaches need to be found. One of these is mild hydrothermal synthesis,[1,2] defined as a reaction occurring in an aqueous medium between 100 °C and the critical temperature of water ($T_c=374.12$ °C) under autogenous pressure. By these means, quite often, laminar, tunnel or cage structures are produced.

On the other hand, molybdenum phosphates involving pentavalent molybdenum represent an interesting family because of their catalytic properties. Until 1983, Mo^V could be considered an unusual valence for molybdenum in oxides, especially in phosphates since only two molybdenum(V) phosphates were known:[3,4] $MoOPO_4$ and $Mo_2P_4O_{15}$. However, in recent years numerous Mo^V phosphates have been discovered,[5–7] some of them only being accessible by hydrothermal synthesis.[8–13]

The phosphate matrix shows a great ability to stabilise pentavalent molybdenum in octahedral coordination forming molybdenyl cations, linked by tetrahedral phosphate groups, contrary to pure octahedral structures for which such isolated Mo^V species are very rarely observed. In addition, for phosphomolybdates the Mo–O bond is off-centred, so that the corresponding oxygen apex is systematically free. As a result, the 'MoPO' framework becomes more flexible, allowing tunnel and cage structures to be synthesised. Because of its open structure, and the pentavalent oxidation state of Mo cations, these materials seem to be good candidates to undergo insertion–extraction reactions.

We have been applying hydrothermal techniques for the synthesis of materials similar to the title phosphomolybdates. The compound $Na_2(MoOPO_4)_2(HPO_4)\cdot 2H_2O$, discovered by Peascoe and Clearfield,[9] shows a structure made up of layers of $MoOPO_4$. The tetragonal $MoOPO_4$ structure contains equal numbers of corner-sharing octahedra and tetrahedra; on the other hand, the O atom of the Mo=O molybdenyl group also forms the long, nearly nonbonded interaction, with the Mo in the next octahedron, and therefore, chains of —Mo—O— with alternating long and short Mo—O distances are generated. The $[(MoOPO_4)_2(HPO_4)]^-$ structure type is related to the $MoOPO_4$ structure by replacing the —O— in the chain by HPO_4. The 3-D structure consists of the $MoOPO_4$-like layers bonded together by hydrogenphosphate groups. The $[(MoOPO_4)_2(HPO_4)]^-$ anionic framework can accommodate both organic and inorganic cations of varying size and shape, the cation variability being accommodated by suitable orientation of the interlamellar phosphate groups.

When the cations are H_3O^+ and Na^+,[9] the compound has a body-centered tetragonal lattice with $a_t\approx 6.4$ and $c_t\approx 16$ Å. The small a dimension results from the four-fold disorder of the interlamellar phosphate groups with the 16 Å spacing corresponding to a two layer sequence. When the cations are Cs^+ and H_3O^+[11] the structure is monoclinic with $a_m\approx b_m\approx 9.1$ and $c_m\approx 16$ Å, a diagonal cell $a_m\approx a_t\sqrt{2}$ and $c_m\approx c_t$ being needed to describe the structure.

Taking into account all these features, it seemed us quite possible that related phosphomolybdates $Na_{2\pm x}(MoOPO_4)_2(HPO_4)\cdot yH_2O$ ($y=2, 0$) could be synthesised by sodium insertion/extraction electrochemical routes. In the present contribution, we report such a synthesis as well as the preliminary structural and magnetic characterisation of these new phosphomolybdates.

Experimental

Synthesis of starting compound

$Na_2(MoOPO_4)_2(HPO_4)\cdot 2H_2O$ was synthesised by hydrothermal treatment of Na_2CO_3, MoO_3, Mo, H_3PO_4 (85%) and H_2O in a mole ratio of 2:1:0.05:20:200 at 250 °C in a similar manner, although not exactly the same, as used by Peascoe and Clearfield.[9] The reaction was carried out in Teflon lined stainless steel containers at autogenous pressure for 96 h followed by slow cooling to 150 °C at *ca.* 1 °C h^{-1}. The

†Basis of the poster presentation given at Materials Chemistry Discussion No. 1, 24–26 September 1998, ICMCB, University of Bordeaux, France.

resulting yellow powder was washed several times with water, rinsed with acetone, and dried in a desiccator at ambient temperature.

The anhydrous compound, $Na_2(MoOPO_4)_2(HPO_4)$ was obtained by thermal treatment of $Na_2(MoOPO_4)_2(HPO_4)\cdot 2H_2O$ at 250 °C during 24 h under vacuum. The resulting green sample was held under an argon atmosphere to avoid the reabsorption of water. In order to evaluate the amount of water lost, the same synthesis procedure was performed in a SEICO 320*U* thermobalance.

Electrochemical synthesis of $Na_{2\pm x}(MoOPO_4)_2(HPO_4)\cdot yH_2O$ ($y=2, 0$)

Electrochemical sodium insertion and extraction reactions from the starting materials were carried out using a Swagelok-type cell bearing metallic sodium as the anode. For the positive electrode a mixture of the corresponding phosphate, carbon black and ethylene–propylene–diene terpolymer (EDPTP) in a 79.5 : 20 : 0.5 ratio was compresed in a 5 mm diameter pellet of approximately 25 mg. For the electrolyte a 1 mol dm^{-3} solution of $NaClO_4$ in propylene carbonate (PC) was used. After assembling the cells in an argon filled glove box, they were connected to a multichannel galvanostatic–potentiostatic system of the 'MacPile' type.

The electrochemical measurements were performed in a stepwise potentiostatic mode with a scan rate of ± 10 mV h^{-1}. The chronoamperometry at each potential level was recorded with a resolution of 0.001 mA h^{-1}.

Preliminary structural characterization

X-Ray powder diffraction patterns of the synthesised compounds were collected using a D-501 power diffraction system, operating at 40 kV and 30 mA with monochromatic Cu-Kα radiation (1.5406 Å). The scan range was $10<2\theta<37°$ with step size of 0.04 and counting time of 14 s.

For dehydrated and electrochemically synthesised compounds, the patterns were collected under an argon atmosphere using a hermetic closed sample holder containing a beryllium window. By using this technique the 2θ scan was limited below 37°.

The AFFMA program was used in order to index the diffraction patterns and to calculate lattice parameters.

Magnetic measurements

The magnetic moments of the samples were measured by SQUID magnetometry. The signal was registered using a field of 0.5 T. After zero field cooling, a magnetic field was applied at 4.2 K, and the measurements were performed up to 200 K.

Results

Starting materials

Fig. 1 shows the powder X-ray diffraction patterns of $Na_2(MoOPO_4)_2(HPO_4)\cdot 2H_2O$. All the Bragg maxima can be indexed based on a tetragonal cell with parameters $a=b=6.43(1)$ Å and $c=15.93(2)$ Å [$V=660.5(3)$ Å^3] in the space group *I*4/*mmm* as previously reported by Peascoe and Clearfield.[9].

Concerning the water-free compound, thermogravimetric analysis results allow us to ensure that two water molecules are lost upon heating $Na_2(MoOPO_4)_2(HPO_4)\cdot 2H_2O$ at 250 °C under vacuum. As shown in Fig. 1, the powder X-ray diffraction pattern of $Na_2(MoOPO_4)_2(HPO_4)$ can be indexed based on a monoclinic cell with parameters $a=9.20(1)$, $b=8.98(2)$, $c=15.71(3)$ Å and $\beta=90.7(2)°$ [$V=1298.9(7)$ Å^3] and was refined to $R_w=0.0027$. This cell was confirmed using selected area electron diffraction experiments.

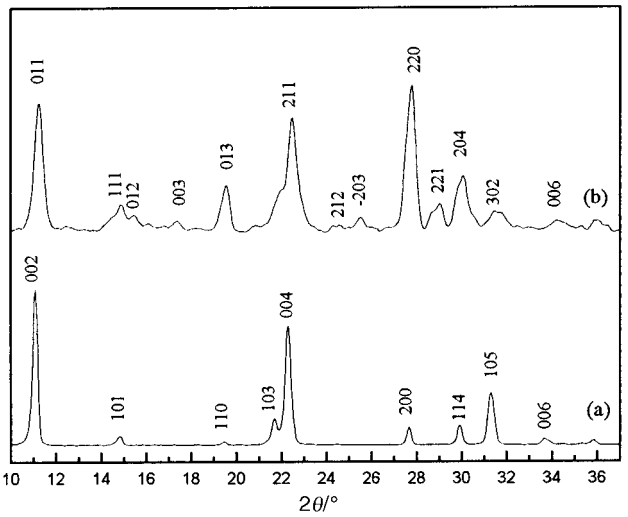

Fig. 1 X-Ray diffraction patterns of (a) $Na_2(MoOPO_4)_2(HPO_4)\cdot 2H_2O$ and (b) $Na_2(MoOPO_4)_2(HPO_4)$.

Electrochemical sodium extraction/insertion

$Na_{2-x}(MoOPO_4)_2(HPO_4)\cdot 2H_2O$ and $Na_{2-x}(MoOPO_4)_2(HPO_4)$. In order to explore the formation of new $Na_{2-x}(MoOPO_4)_2(HPO_4)\cdot 2H_2O$ phases a cell of configuration sodium|electrolyte|$Na_2(MoOPO_4)_2(HPO_4)\cdot 2H_2O$ was charged up to 4 V *vs.* Na^+/Na, as limited by the stability of the electrolyte. The variation of the cell voltage during the charge process *vs.* the amount of extracted sodium is shown in Fig. 2(a). At the final voltage, 4 V, the composition of the active material $Na_{2-x}(MoOPO_4)_2(HPO_4)\cdot 2H_2O$ corresponds to the extraction of 0.68 sodium ions from the starting material. Preliminary information about the mechanism of the extraction process is obtained from the incremental capacity curve, dx/dV also plotted in Fig. 2(a). This curve exhibits a broad minimum at *ca.* 3.6 V *vs.* Na^+, indicating that a phase transition occurs at this voltage during the extraction process.

The nature of this phase transition can be clarified from the variation of the cell current intensity *vs.* time.[14] In this way, the corresponding chronoamperogram, shown in Fig. 2(b), with a quite different current decay in both sides of the minimum, is characteristic of a first order phase transition.[15] From this experiment we can now infer that for the composition $0<x<0.4$ the system is in a two-phase region where the initial compound and a new solid solution coexist. Therefore, a $Na_{2-x}(MoOPO_4)_2(HPO_4)\cdot 2H_2O$ solid solution exists at least in the compositional range $0.4<x<0.68$. With the aim of studying this new solid solution phase, the pellet of the final product $Na_{1.32}(MoOPO_4)_2(HPO_4)\cdot 2H_2O$ was removed from the cell and used for preliminary structural characterisation.

In order to study the reversibility of the extraction process, another cell of the same configuration was charged and consecutively discharged down to the initial open circuit voltage value and results are presented in Fig. 2(c) as voltage–composition and intensity–voltage representations (insert), respectively. From both plots, it is clear that the material $Na_2(MoOPO_4)_2(HPO_4)\cdot 2H_2O$ can reversibly undergo sodium extraction reaction in the studied voltage window. Additionally, the reversibility of the reaction gives us an idea of the close structural relationships between the two phosphomolybdates $Na_2(MoOPO_4)_2(HPO_4)\cdot 2H_2O$ and $Na_{1.32}(MoOPO_4)_2(HPO_4)\cdot 2H_2O$ which is confirmed by XRD.

This experiment was repeated but using the anhydrous compound $Na_2(MoOPO_4)_2(HPO_4)$ as the active material. Fig. 3(a) and (b) show the results of charging a cell of configuration sodium|electrolyte|$Na_2(MoOPO_4)_2(HPO_4)$ up to 4 V *vs.* Na^+/Na. As for $Na_{2-x}(MoOPO_4)_2(HPO_4)$ the

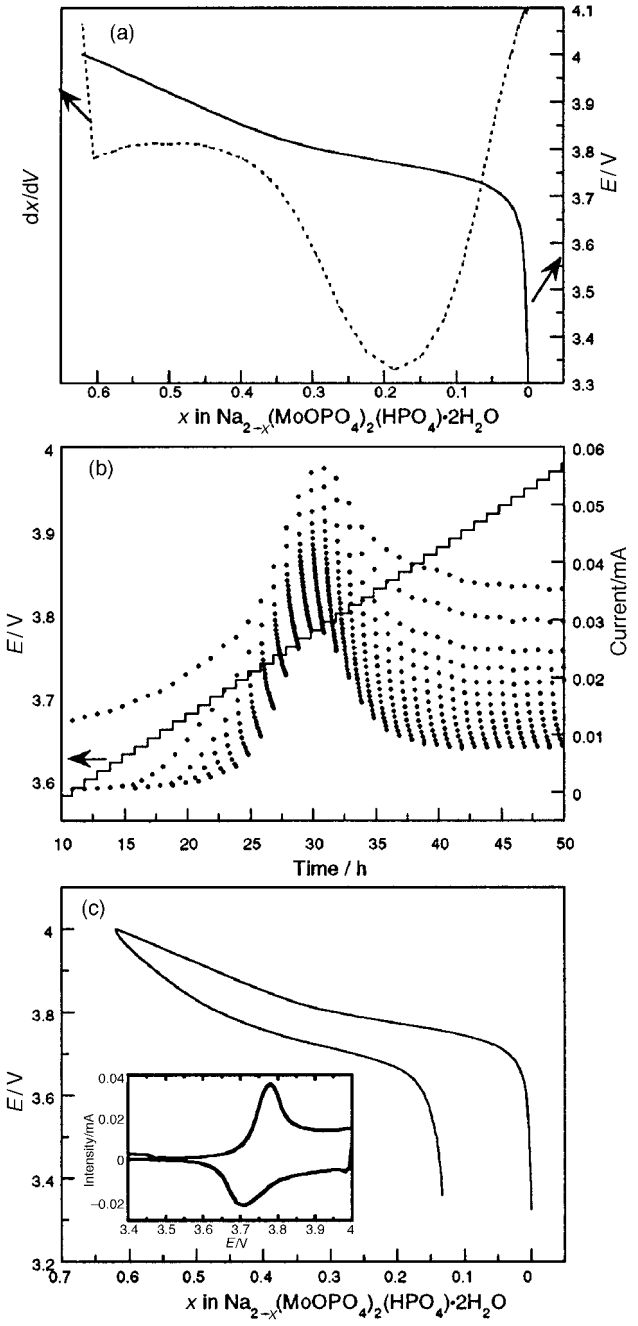

Fig. 2 Electrochemical extraction study of $Na_2(MoOPO_4)_2(HPO_4)\cdot 2H_2O$. (a) Representation of voltage and incremental capacity curves *vs.* the degree of extracted sodium. (b) Time dependence of the current. (c) Consecutive charge and discharge cicles.

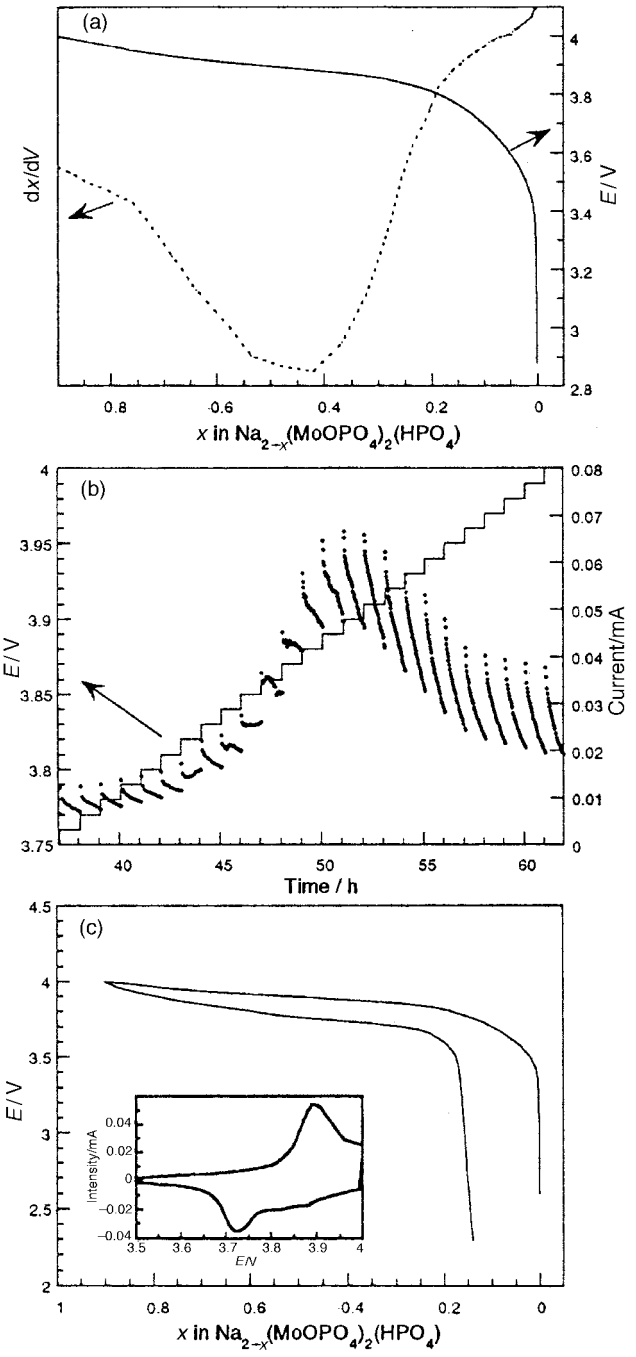

Fig. 3 Result of the first charge of a cell sodium|$NaClO_4$+PC|$Na_2(MoOPO_4)_2(HPO_4)$. (a) Representation of voltage and incremental capacity curve *vs.* the degree of deinsertion. (b) Variation of the intensity current with time during the first charge of the cell. (c) Charge and discharge plots.

extraction reaction proceeded through a first order transition which in this case leads to the formation of a solid solution $Na_{2-x}(MoOPO_4)_2(HPO_4)$ with $0.75<x<1$. The upper limit of this new solid solution, $Na(MoOPO_4)_2(HPO_4)$ was used for structural characterisation.

To study the reversibility of the extraction reaction leading to the solid solution $Na_{2-x}(MoOPO_4)_2(HPO_4)$ with $0.75<x<1$ another cell of the same configuration was charged and discharged in the voltage range 3.3–4.0 V. As can be seen in Fig. 3(c) the voltage–composition curves for the charge and discharge processes have similar paths and shapes, which means that the extraction reaction is reversible. This is also noticeable in the voltage–intensity representation [Fig. 3(c), insert].

If now we compare the behaviour of $Na_2(MoOPO_4)_2(HPO_4)\cdot 2H_2O$ and $Na_2(MoOPO_4)_2(HPO_4)$, the amount of extracted sodium is only slightly higher in the water free compound. Therefore, it seems that in the studied voltage range the molecules of water are not disturbing the removal of sodium atoms from the structure. Moreover, the general features of the extraction reaction in both compounds are equivalent, independently of the water content.

$Na_{2+x}(MoOPO_4)_2(HPO_4)\cdot 2H_2O$ and $Na_{2+x}(MoOPO_4)_2(HPO_4)$. In the opposite direction new, sodium richer phases, $Na_{2+x}(MoOPO_4)_2(HPO_4)\cdot yH_2O$ ($y=2$, 0) can also be obtained through the electrochemical route. With this aim sodium cells using the phosphomolybdates as active material were discharged down to 1 V *vs.* Na^+/Na.

Fig. 4(a) shows the voltage–composition curve obtained from the discharge of a cell sodium|electrolyte|

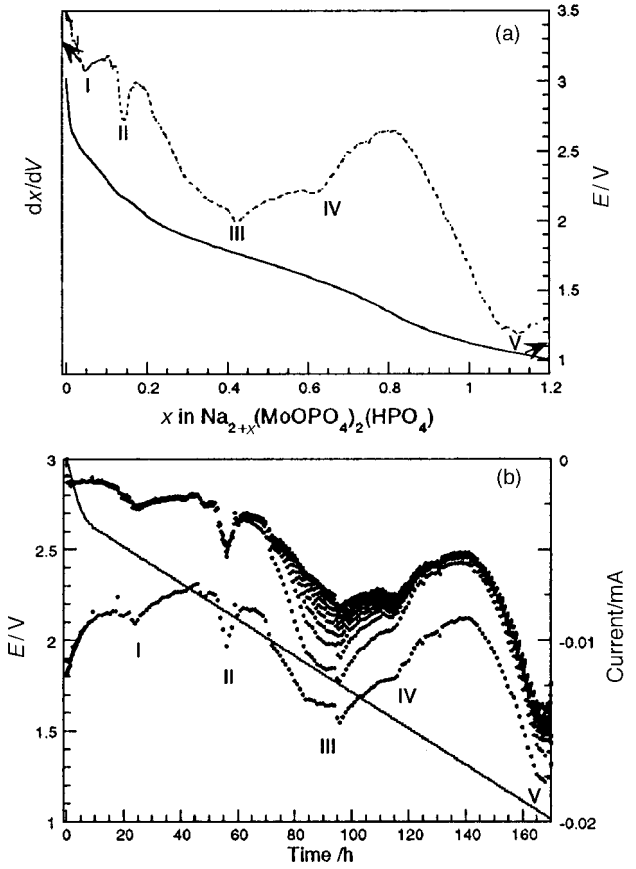

Fig. 4 Result of the first discharge of a sodium|$NaClO_4$+PC|$Na_2(MoOPO_4)_2(HPO_4)\cdot 2H_2O$ cell. (a) Plot of voltage and incremental capacity curve *vs.* composition. (b) Time dependence of the current with 10 mV voltage steps.

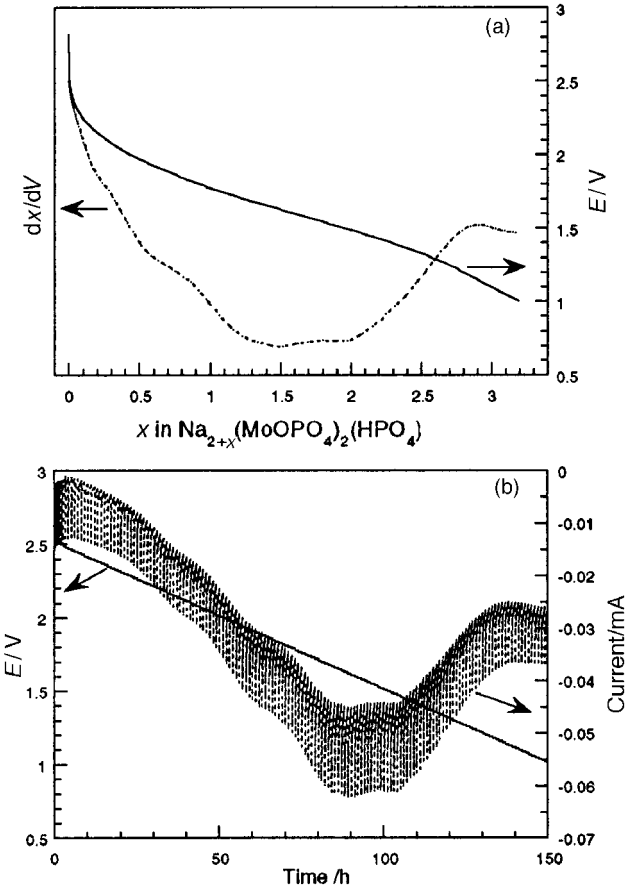

Fig. 5 Electrochemical sodium insertion in $Na_2(MoOPO_4)_2(HPO_4)$. (a) Representation of voltage and incremental capacity curve *vs.* the amount of inserted sodium and (b) variation of the intensity current with time during the first discharge of the cell.

$Na_2(MoOPO_4)_2(HPO_4)\cdot 2H_2O$ and for a better visualization of the involved processes the derivative curve, dx/dV, is also plotted. In the derivative curve five minima consecutively labelled as I–V appear, indicating that the insertion reaction involves five phase transitions, which in nature could, in principle, be investigated through the respective chronoamperograms. However, as can be seen in Fig. 4(b), for processes I–III the data are not sufficiently well resolved so as to ensure the order of the phase transitions.[16] For the phase transitions IV and V, the variation of the intensity current *vs.* time is characteristic of a first order transition.[14] This means that the region in between both first order transitions is a single phase $Na_{2+x}(MoOPO_4)_2(HPO_4)\cdot 2H_2O$, for which approximate composition limits, as estimated from Fig. 4(a), are $0.75<x<0.9$. To study the structure of this solid solution a cell of the same configuration was discharged limiting the degree of insertion up to $x=0.9$, and the pellet of the phase $Na_{2.9}(MoOPO_4)_2(HPO_4)\cdot 2H_2O$ was studied by XRD.

The result of the experiment carried out using $Na_2(MoOPO_4)_2(HPO_4)$ as active material is shown in Fig. 5. During the first discharge of this cell, the material can accept 3.2 sodium ions in its structure, which is more than twice the amount inserted in the compound $Na_2(MoOPO_4)_2(HPO_4)\cdot 2H_2O$. In this case, and contrary to what is seen in the extraction process, the behaviour of both compounds is quite different. Obviously, water removal from the tunnel results in new available positions for inserting sodium: the lower the water content, the higher the capacity becomes. Concerning the processes involved during the insertion reaction in $Na_2(MoOPO_4)_2(HPO_4)$, only one phase transition has been detected in the incremental capacity curve. However, the minima in the related chronoamperogram [Fig. 5(b)] display associated shoulders that could be produced from superimposing processes. Nevertheless, a $Na_{2+x}(MoOPO_4)_2(HPO_4)$ solid solution exists in the composition range $2.6<x<3.2$, and a representative example, $Na_{4.7}(MoOPO_4)_2(HPO_4)$, has been synthesised and used for structural characterisation.

Preliminary structural characterization of the new $Na_{2\pm x}(MoOPO_4)_2(HPO_4)\cdot yH_2O$ ($y=2, 0$) phases

The X-ray diffraction patterns of the new sodium inserted and extracted compounds obtained from water containing material are plotted in Fig. 6, while the patterns corresponding to the water free phosphomolybdate are shown in Fig. 7. All patterns can be indexed based on a monoclinic cell ($a_m\approx b_m\approx a_t\sqrt{2}$ and $\beta\neq 90^\circ$), which is diagonal with regard to the former tetragonal cell; corresponding to the starting, water-containing phosphomolybdate. This modification of the symmetry is due to a reorientation of the interlayer phosphate groups which occurs, either by changing the sodium content or by elimination of water.

Since no large differences were observed in either the position or intensity of the reflections with sodium content, it seems that all the $Na_{2\pm x}(MoOPO_4)_2(HPO_4)\cdot yH_2O$ ($y=0, 2$) phases are isostructural. However the unit cell parameters (Table 1) indicate that the introduction of a higher amount of sodium cations produces an expansion of the unit cell. Clearly all the phases have the same framework structure. Further investigation will be needed in order to fully determine the structure of these new phosphomolybdates.

Magnetic properties

The process of insertion and extraction in the hydrated material can be followed by magnetic susceptibility measurements. The

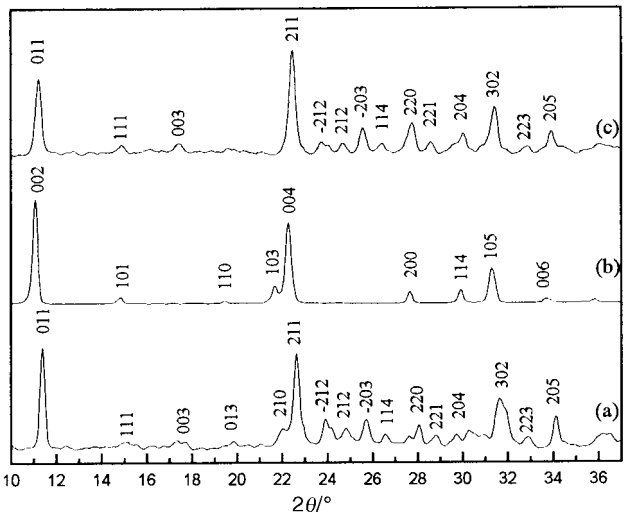

Fig. 6 X-Ray diffraction patterns of the $Na_{2+x}(MoOPO_4)_2(HPO_4)\cdot 2H_2O$ compounds with (a) $x=-0.68$, (b) $x=0$ and (c) $x=0.9$.

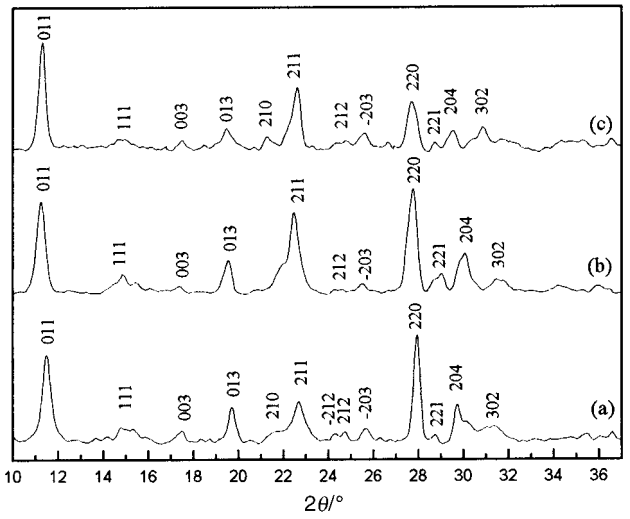

Fig. 7 X-Ray diffraction patterns of the compounds $Na_{2+x}(MoOPO_4)_2(HPO_4)$ with (a) $x=-1$, (b) $x=0$ and (c) $x=2.7$.

Table 1 Cell parameters for $Na_{2+x}(MoOPO_4)_2(HPO_4)\cdot 2H_2O$ phases

x	y	a/Å	b/Å	c/Å	β/°	V/Å^3	R_w
−0.68	2	9.09(2)	8.92(2)	16.02(5)	90.4(2)	1299.0(9)	0.0042
0	2	9.09(1)	9.09(1)	15.93(2)	90	1320.8(3)	0.0022
0.9	2	9.09(4)	9.01(3)	16.14(6)	90.5(3)	1322(2)	0.0050
−1	0	9.15(1)	8.89(1)	15.67(2)	91.1(1)	1274.9(5)	0.0019
0	0	9.20(1)	8.98(2)	15.71(3)	90.7(2)	1298.9(7)	0.0031
2.7	0	9.31(3)	8.82(4)	15.90(5)	90.8(3)	1304(1)	0.0057

starting material, where Mo^V, a d^1 paramagnetic cation is present, shows a typical Curie–Weiss behaviour down to 4.2 K, as can be seen in Fig. 8 where $1/\chi$ *vs.* T has been plotted. The effective spin only magnetic moment calculated from this plot is 1.84 μ_B per Mo atom, which is close to the theoretical value (1.73 μ_B). For sodium extracted materials, the oxidation to Mo^{VI}, a d^0 diamagnetic cation, can also be followed by these means. Curie–Weiss behaviour is also observed in the $1/\chi$ *vs.* T plot corresponding to these materials. As an example, Fig. 8 shows the plot of an oxidized phase whose stoichiometry, as deduced from the voltage–composition measurements, is 1.32 sodium per formula unit, corresponding to 0.68 Mo^{VI} and 1.32 Mo^V. The effective spin only magnetic moment calculated from this plot is lower than that before the extraction, $\mu_{eff}=$ 1.65 μ_B per Mo atom and the agreement with the theoretical value taking into account the individual contributions of Mo^V and Mo^{VI} is almost perfect.

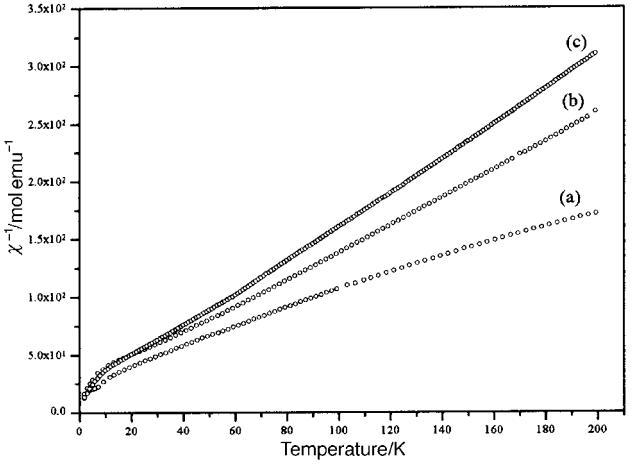

Fig. 8 $1/\chi$ *vs.* temperature for the $Na_{2+x}(MoOPO_4)_2(HPO_4)\cdot 2H_2O$ compounds with (a) $x=0.9$, (b) $x=0$ and (c) $x=-0.68$.

Fig. 8 also shows the $1/\chi$ *vs.* T plot for a sodium inserted material corresponding to a reduced phase the stoichiometry of which, as deduced from the voltage–composition measurements, is 2.9 sodium ions per formula unit, which would correspond to 0.9 Mo^{IV} and 1.1 Mo^V per formula unit. The effective spin only magnetic moment calculated from this plot is higher than found before the insertion, $\mu_{eff}=2.31$ μ_B per Mo atom and the agreement with the theoretical value taking into account the individual contributions of Mo^{IV} and Mo^V is also very good.

Concluding remarks

This contribution is an example of how a sodium phosphomolybdate obtained by hydrothermal synthesis can be used as a matrix for both intercalation/extraction electrochemical reactions. As we have shown, the combination of these two soft chemistry techniques opens exciting avenues to obtain new metastable compounds, the properties of which can be quite different from the original.

This work has been possible thanks to a Complutense grant awarded to M.E.A. and financial support from the Spanish Ministery of Education (CICYT, Project MAT95-0809).

References

1 A. Rabenau, *Angew. Chem., Int. Ed. Engl.*, 1985, **24**, 1026.
2 M. S. Whittingham, *Curr. Opin. Solid State Mater. Sci.*, 1996, **1**, 227.
3 P. Kierkegaard and J. M. Longo, *Acta Chem. Scand.*, 1970, **24**, 427.
4 L. K. H. Minacheva, A. S. Antsyshkina, A. V. Lavrov, V. G. Sakharova, V. P. Nikolaev and M. A. Porai-koshits, *Russ. J. Inorg. Chem.*, 1979, **24**, 51.
5 R. C. Haushalter and L. A. Mundi, *Chem. Mater.*, 1992, **4**, 31.
6 A. Leclaire, T. Hoareau, M. M. Borel, A. Grandin and B. Raveau, *J. Solid State Chem.*, 1995, **114**, 543.
7 S. Ledain, A. Leclaire, M. M. Borel and B. Raveau, *J. Solid State Chem.*, 1997, **132**, 249.
8 L. A. Mundi and R. C. Haushalter, *Inorg. Chem.*, 1990, **29**, 2879.
9 R. Peascoe and A. Clearfield, *J. Solid State Chem.*, 1991, **95**, 289.
10 R. Peascoe and A. Clearfield, *J. Solid State Chem.*, 1991, **95**, 83.
11 L. A. Mundi, l. Yacullo and R. C. Haushalter, *J. Solid State Chem.*, 1991, **95**, 283.

12 H. E. King, L. A. Mundi, K. G. Strohmaier and R. C. Haushalter, *J. Solid State Chem*., 1991, **92**, 1.
13 A. Leclaire, C. Biot, H. Rebbah, M. M. Borel and B. Raveau, *J. Mater. Chem*., 1998, **8**, 439.
14 Y. Chabre, *NATO ASI Ser.*, 1993, **305**, 181.
15 G. B. M. Vaughan, M. Barral, T. Pagnier and Y. Chabre, *Synth. Met.*, 1996, **77**, 7.
16 A. H. Thompson, *J. Electrochem. Soc*., 1979, **126**, 608.

Paper 8/06498I